$O^{16}(\gamma,n)O^{15}$ Cross Section from Threshold to 65 MeV*

B. C. Cook, J. E. E. Baglin,† J. N. Bradford, and J. E. Griffin
Iowa State University, Ames, Iowa

(Received 13 May 1965; revised manuscript received 9 August 1965)

The $O^{16}(\gamma,n)O^{15}$ cross section has been measured using least-structure analysis of photonuclear yield functions for energy to 65 MeV. In the giant-resonance energy region considerable structure is reported, in good agreement with structure reported using other methods. The resolution of the least-structure method is comparable to resolution obtained by other methods, and in certain energy regions is superior. The cross section extends to energy above the giant resonance, exhibiting prominent structure to the highest energy measured. Absolute cross sections are reported in good agreement with values obtained elsewhere from yield functions, but approximately 20% higher than measurements made using monochromatic photons.

I. INTRODUCTION

STRUCTURE in the giant resonance of photonuclear reactions for the light elements is now well established experimentally. In O^{16} the strongest transitions seem to be correlated with the $E1$ transitions of the one-particle–one-hole model of Brown and others,[1–4] although the relative strengths among the various transitions as well as the absolute cross sections deviate from the theory. In particular, the five $E1$ particle-hole transitions exhaust the $E1$ sum rule in the Brown model, while the experimentally observed cross section is well below this limit. Thus high-energy processes must be an important fraction of the total $E1$ strength. While the quasideuteron process[5,6] certainly contributes an appreciable fraction of the high-energy strength, harmonics of the giant resonance itself have been suggested as a possible alternative high-energy mechanism.[7,8]

Since electron accelerators provide a bremsstrahlung spectrum of photons, much of the early work in photonuclear cross-section measurement was based upon analysis of photonuclear yield functions. A photonuclear yield is the number of photonuclear transitions (as evidenced by detection of the resulting nucleons or by counting the resultant radioactivity) per unit incident energy at a particular bremsstrahlung energy. A yield function is a sequence of yields as a function of energy. Analysis of yield functions[9] without smoothing fails to give statistically meaningful cross sections above the giant resonance, because of experimental errors in the yield functions. Other techniques for the study of photonuclear cross sections at higher energies have given only limited results. Thus our knowledge of the photonuclear cross section above 30 MeV is fragmentary. A new method for the analysis of photonuclear yield functions was recently proposed.[10] The effective resolution of the method, "the least structure method" (LS) is adequate to resolve structure in the photonuclear cross section above the giant resonance. Since structure is well developed in the giant resonance of O^{16} and the cross section is reasonably described by a simple theory, the $O^{16}(\gamma,n)O^{15}$ process was selected for study.

While the initial motivation of this work was the search for structure above the giant resonance,[11] experience with (LS) has shown that the resolution is comparable to direct methods for studying photonuclear reactions as currently reported. Because of the considerable experimental and theoretical interest in the giant-resonance region in O^{16}, measurements were also made in smaller energy intervals at lower energies. This work supplements the time-of-flight measurements of neutron spectra,[12,13] the interpretation of which is complicated by the possibility of non-ground-state transitions, and complements the recent measurements using monochromatic γ-ray sources.[14,15] Accurately determined yield functions must be obtained in order to derive reliable cross-section values. Small systematic errors concentrated in local energy intervals can produce spurious resonances in the cross sections. The accuracy of the yield function, as measured by the reproducibility of the measurements at a fixed energy, should be better than 1%, and preferably 0.3% to achieve resolutions sufficiently narrow to resolve structure in the photonuclear cross section by the (LS) method. To insure reliable yield functions and to achieve the required reproducibility, many precautions

* Work was performed at Ames Laboratory of the U. S. Atomic Energy Commission.

† Present address: Electron Accelerator Laboratory, Yale University, New Haven, Connecticut.

[1] G. E. Brown and M. Bolsterli, Phys. Rev. Letters **3**, 472 (1959).

[2] G. E. Brown, L. Castillejo, and J. A. Evans, Nucl. Phys. **22**, 1 (1961).

[3] V. Gillet and N. Vinh Mau, Phys. Letters **1**, 25 (1962).

[4] J. P. Elliott and B. H. Flowers, Proc. Roy. Soc. (London) **A242**, 57 (1957).

[5] J. S. Levinger, Phys. Rev. **84**, 43 (1951).

[6] A. Wattenberg, A. C. Odian, P. C. Stein, R. M. Weinstein, and H. Wilson, Phys. Rev. **104**, 1710 (1956).

[7] J. H. Carver, D. C. Peaslee, and R. B. Taylor, Phys. Rev. **127**, 2198 (1962).

[8] M. Danos, Ann. Physik **10**, 265 (1952).

[9] A. S. Penfold and J. E. Leiss, Phys. Rev. **114**, 1332 (1959).

[10] B. C. Cook, Nucl. Instr. Methods **24**, 256 (1963).

[11] D. W. Anderson, A. J. Bureau, B. C. Cook, J. E. Griffin, J. McConnell, and K. Nybö, Phys. Rev. Letters **10**, 250 (1963).

[12] F. W. K. Firk, Nucl. Phys. **52**, 437 (1964).

[13] P. F. Yergin, R. H. Augustson, N. N. Kaushal, H. A. Medicus, W. R. Moyer, and E. J. Winhold, Phys. Rev. Letters **12**, 733 (1964).

[14] J. Miller, C. Schuhl, G. Tamas, and C. Tzara, Phys. Letters **2**, 76 (1962).

[15] R. L. Bramblett, J. T. Caldwell, R. R. Harvey, and S. C. Fultz, Phys. Rev. **133**, B869 (1964).

were taken and independent checks of the procedure made. Since this work is the first of a series of cross-section measurements in various elements in which (LS) analysis will be used, our procedure to guarantee reliable yield functions will be described here in some detail.

II. REACTION YIELD DATA

Data were obtained on the reaction $O^{16}(\gamma,n)O^{15}$ by irradiating oxygen samples (compressed HBO_3) with bremsstrahlung photons from the Iowa State University 70-MeV synchrotron. Electrons accelerated in the synchrotron were deflected into a 0.01-in.-thick tungsten target at precisely known energies. The resulting photon beam was passed through a 25-cm tapered lead collimater, through the oxygen sample, and into an NBS-type P2 ionization chamber.[16] The experimental geometry is shown in Fig. 1. The energy intervals employed were (1) 125-keV intervals from 15.5 to 30.375 MeV, (2) 250-keV intervals from 30.375 to 45.25 MeV, and (3) 500-keV intervals from 45.25 to 65.5 MeV. The $O^{16}(\gamma,n)O^{15}$ process was detected by counting the 0.51-MeV annihilation photons emitted in the subsequent 2-min positron decay of O^{15}. Samples were irradiated for 3 min, 1 min was allowed to elapse during which the sample was removed to the radioactivity counting system, and then the annihilation photons from O^{15} were counted for 3 min. The counting system consisted of two 3-in.-by-3-in. NaI(Tl) scintillating crystals mounted face to face with the sample between them. The photomultiplier tubes were EMI-type 9531B and each tube was powered by aspectrum-stabilizing feedback power-supply system. Temperature-compensated tunnel diodes were used as integral discriminators in the counting systems. Above 28 MeV more than 1.5 million counts were obtained in each counter for each datum. At high counting rates ($\sim 10^4$/sec) a shift in detection efficiency with counting rate was observed. The effect was determined empirically by measuring the 20-min half-life of C^{11} produced by bombardment of a C^{12} target at an energy below the $(\gamma,2n)$ threshold energy of 32 MeV. The deviation from a pure exponential decay was used to generate an empirical count-rate correction factor. Maximum corrections due to counting loss were always less than 4%.

The 3-min bombardment, 1-min wait, and 3-min counting time were all controlled by scalers counting the line frequency, which was checked against WWV.

During each counting period the next succeeding sample was irradiated at a new energy. Irradiation energies were selected at random from a card file of all energies required for a given yield curve. This manner of energy selection precludes the introduction of erroneous structure into a yield curve as a result of time-varying drifts in equipment.

[16] J. S. Pruitt and S. R. Domen, Natl. Bur. Std. (U. S.) Monograph 48, (1962).

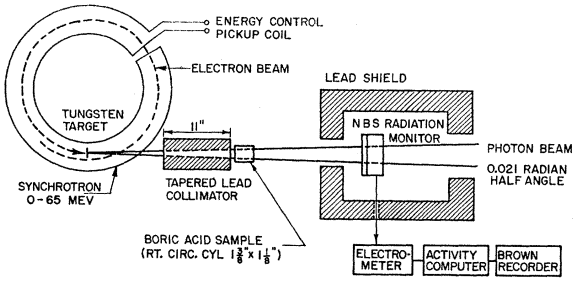

FIG. 1. Experimental arrangement for sample bombardment. The sample is bombarded in eclipsing geometry for 3 min, transported manually, and then counted for 3 min using two 3-in. NaI(Tl) scintillation counters located away from the synchrotron.

The production rate $P(E_0,t)$ for O^{15} at a time t at an electron energy E_0 is related to the cross section by

$$P(E_0,t)=N_0\int_{E_{\rm th}}^{E_0}\sigma(k)\frac{dN}{dk}(E_0,k,t)dk. \qquad (1)$$

The symbols have the following meaning:

N_0, number of O^{16} atoms per square centimeter in the photon beams;

k, photon energy in MeV;

$dN(E_0,k,t)/dk$, photons per MeV per second striking the sample;

$\sigma(k)$, reaction cross section;

$E_{\rm th}$, reaction threshold energy.

In Eq. (1) integration of the photon beam over the collimated solid angle subtended by the sample is assumed. Since both the samples and the monitoring ionization chamber were larger than the collimated photon beam (Fig. 1), fluctuations in yield due to position errors in the sample or effective-solid-angle changes due to variation in beam properties (beam width or position, etc.) were minimized.

Ionization current was measured using a Cary model 31 electrometer with a 100-MΩ resistor in parallel with a 0.001-μF capacitor. The resistor was maintained to ±1°C in a crystal oven and the output current of the ionization chamber was to be kept below 2×10^{-8} A. Thus variation in sensitivity due to temperature changes of the resistor was below 0.1%. With a maximum drop of 2 V across the input resistor the nonlinearity was below 0.1%. In this configuration the output voltage of the electrometer is proportional to the instantaneous photon flux incident upon the ionization chamber. For electron energy E_0, the output voltage of the electrometer can be related to the flux of photons by

$$V(E_0,t)=\alpha\int_0^{E_0}\frac{dN}{dk}(E_0,k,t)M(k)dk, \qquad (2)$$

where, again, integration over the beam solid angle is assumed.

$M(k)$ is the ionization chamber response in coulombs

for a single photon of energy k entering the chamber[16] and α is a proportionality factor depending on the electrometer feedback resistor.

The ionization chamber was surrounded with a lead wall 8 or more in. thick. When the beam was stopped by 8 in. of lead the monitor current was reduced by a factor 3×10^{-4}, consistent with the calculated photon attenuation. The presence of the lead wall changed the effective geometry of the monitor from that used by the National Bureau of Standards in measuring its absolute sensitivity. An auxiliary experiment was made to test this effect as a function of synchrotron energy. No detectable deviation was found between the two geometries. The P2 chamber was slightly modified from the National Bureau of Standards design so that a small positive pressure of filling gas could be maintained and no temperature or pressure corrections were necessary. Since the beam striking the monitor is modified by electronic absorption in the sample ($\sim$0.1 attenuation lengths), the transmission of the sample was measured as a function of synchrotron energy. The transmission varied from 0.85 at 15.5 MeV to 0.90 at 65 MeV. Sample absorption correction factors were then applied to the monitor response at each energy.

Since O^{15} is radioactive with decay constant λ, the number R of radioactive O^{15} nuclei in the sample after a bombarding time t is related to $P(E_0,t)$ by the differential equation

$$dR(E_0,t)/dt+\lambda R(E_0,t)=P(E_0,t). \quad (3)$$

In Eqs. (1) and (2), $dN(E_0,t)/dk$ is not necessarily constant in time. For this reason the electrometer output voltage $V(E_0,t)$ was delivered to an electronic circuit, the response of which was the analog of equation (3).[17] The response of the circuit is described by the equation

$$dA(t)/dt+\lambda A(t)=aV(E_0,t), \quad (4)$$

where a is a constant of proportionality. The output voltage of such a circuit is proportional to the irradiated-sample radioactivity at any time t. Zero drift was checked frequently during the experiment and was kept below 0.1% of the smallest activity recorded.

The experimental yield function $Y(E_0)$ at the end of a bombardment T is

$$Y(E_0)=\frac{\text{No. of counts detected}}{A}=\frac{\eta}{A}\int_{t_1}^{t_2}\frac{dR}{dt}dt, \quad (5)$$

where t_1 and t_2 are the times counting begins and ends and η is the counter efficiency. $Y(E_0)$ was found to be independent of the synchrotron intensity after corrections were made for counting losses.

Before an analysis of the experimental yield is possible, numerous small corrections must be made to the data, and to ensure the reliability of interpretation many experimental precautions must be taken. Frequently without these precautions the resulting yield function will not be reproducible, and even if it is, the derived cross section will be unreliable. The precautions necessary to ensure reliable yield functions are best made in terms of the Eqs. (1)–(5) defining the experimental photonuclear yield function $Y(E_0)$.

Significant factors in Eqs. (1)-(5) can be seen to include: (1) N_0, the number of nuclei/cm^2 in the beam, (2) E_0, the electron energy, (3) $dN(E_0,k,t)/dk$, (4) $\sigma(k)$, the cross section, (5) $M(E_0)$, the monitoring response function, and (6) ϵ, the detection efficiency. Each of the above factors must be known and constant in time. And unless irrelevant experimental factors such as monitor zero shift and counting backgrounds are removed, the interpretation of $Y(E_0)$ as a photonuclear yield function is erroneous. Precautions taken to ensure the reliability and stability of each of the above factors will be considered briefly.

1. N_0, the Number of Atoms per Square Centimeter Irradiated

Thirty-five cylindrical oxygen samples $1\frac{1}{8}$ in. in diameter by $1\frac{3}{8}$ in. in length were made by compressing analytically pure boric acid in a powder press. Although the initial amount of boric acid used was kept constant, small variations in the final weight of the samples were detected. Also the density of the samples fluctuated to a small extent and presumably was not uniform throughout the samples. For these reasons the samples were bombarded and counted with a fixed orientation to eliminate fluctuations due to angular asymmetry in the counting efficiency. Also each sample was bombarded three or more times at 36.00 MeV and these results were used to normalize the samples. The largest sample-normalization corrections were 1%.

2. Electron Energy E_0

The energy of the electrons producing the bremsstrahlung is perhaps the most significant parameter affecting a yield curve. The electrons must be as monoenergetic as possible and the energy must be reproducible with known absolute value. The accelerator electron energy is determined continuously by an analog computer. The system is described extensively elsewhere.[18] Essentially, a time-dependent voltage is created which is the analog of the instantaneous value of the electron energy. This voltage is compared with a dc reference voltage so that when the voltages become equal the electrons are deflected onto an internal target. The sensitivity is such that a 4-keV energy shift is easily detected and may be manually corrected. The stability of the reference voltage is better than 0.01% or ±7 keV indefinitely.

The energy scale was determined using the 17.28-

[17] R. L. Garwin, Rev. Sci. Instr. **21**, 411 (1950).

[18] J. E. Griffin and Charles Hammer, U. S. Atomic Energy Commission Report IS-676, 1964 (unpublished).

MeV [19] level in O^{16} and the time the synchrotron field goes through zero. The 17.28-MeV level is apparent in our data as a strong break in the activation curve. The short- and long-term stability of the voltage corresponding to this break is reproducible to ± 3 mV. Three millivolts will correspond to long- and short-term stability at 17.28 MeV of ± 6 keV, and represents our ability to measure energy and not the ultimate limitation of the equipment.

The linearity of the energy scale was checked at 10.83 MeV using the $Cu^{63}(\gamma,n)Cu^{62}$ threshold,[20] which fell on our linear momentum scale. Beyond 17.28 MeV the scale was assumed to be linear to 65 MeV. Since the structure reported here in the giant-resonance region agrees well with that reported in other laboratories, this agreement justifies the extrapolation to about 27 MeV. Beyond 30 MeV no convenient energy calibration points exist, so that an independent check of the scale has not been made. The output voltage of the energy-control system is, however, known to be linear in response to a constant stimulus over the entire range of output voltage.

In order to examine the effect of the energy control system upon measured cross section above 30 MeV, the constant of proportionality relating the output voltage to the true energy was changed and a new set of yield curves measured. No change in the cross-section structure above 30 MeV was observed, whereas if nonlinearity existed in either the energy control system or the dc voltage reference supply, such a change would have changed the appearance of the measured cross section. As a further check on the operation of the energy control system, the synchrotron magnet excitation was reduced 30%. The output voltage corresponding to the 17.28-MeV break remained the same.

3. Photon Spectrum Considerations, dN/dk

In analysis of data the bremsstrahlung spectrum was assumed to be the Schiff integrated-over-angle thin-target spectrum.[21,22] This represents a compromise between a true thin-target spectrum and one resulting from slight multiple scattering in the target. Data were also analyzed using slight modifications of spectrum, with results to be described later.

Variations in the beam direction constitutes a serious problem in acquisition of high-quality yield data. If the center position of the beam were a function of the energy E_0 the effective spectra would change because bremsstrahlung depends upon angle. More seriously, perhaps, the collimator would no longer be aligned, so that low-energy photons and electrons would be produced by edge scattering off the ends of the collimator. This would effectively degrade the spectrum from the assumed bremsstrahlung type. Typically, beam swing is a resonance effect within the accerator appearing discontinuously above a fixed energy. The exact energy of the discontinuity tends to change as a function of time as the magnetic properties of the accelerator change. In our accelerator such effects are frequently observed, but by a careful compromise between rf frequency—i.e., equilibrium orbit position—and target position, beam "swing" can be eliminated. The central position of the beam can be measured to within ± 0.3 mm by activation of small copper disks both in a vertical and horizontal plane. The position of this maximum does not move within experimental errors between 20 and 65 MeV when adjustments are proper. These measurements are repeated periodically during the course of an experiment to ensure their continued validity.

The copper activation used to check beam position also gives the effective angular distribution of the beam at various energies. This distribution is consistent with the multiple scattering in the 0.01-in. tungsten target.

4. Cross Section $\sigma(k)$

Detected events can arise from any nuclear process leading to a radioactive nuclide other than O^{15}. Thus yield due to extraneous processes must be subtracted from the observed yields. No detectable radioactive decays arise from boron and no effects due to impurities were seen. However, above 30 MeV longer lived activities arising from $O^{16}(\gamma,\alpha n)C^{11}$ ($T_{1/2}=20$ min) and $O^{16}(\gamma,2pn)N^{13}$ ($T_{1/2}=10$ min) were observed. A coarse yield function was made for these activities by the analysis of the radioactive decay curves as a function of synchrotron energy. The maximum correction applied was 1.5%. Another competing process is $O^{16}(\gamma,2n)O^{14}$ ($T_{1/2}=72$ sec). No correction was made for this process, but the bombardment time of 3 minutes, combined with the wait of one minute, would reduce its importance relative to the 2-min O^{15} decay. No evidence for the 2.3-MeV γ ray in the 70-sec O^{14} decay was observed at any energy.

5. Energy Response of the P2 Ionization Chamber, $M(E_0)$

Before an experimental yield curve which is monitored per coulomb of collected ionization can be analyzed for the cross section, the calibration of the ionization chamber must be known. The National Bureau of Standards monograph[16] describing the energy response of a type P2 chamber gives two extreme limits for the energy response as well as the average response. Cross sections were derived using both extreme response functions. Although the derived cross sections differ in minor ways, the structure remains essentially unchanged for these modified yield functions.

[19] K. N. Geller and E. G. Muirhead, Phys. Rev. Letters **11**, 371 (1964).
[20] F. Everling, L. Koenig, J. Mattauch, and A. H. Wapstra, in *1960 Nuclear Data Tables* (U. S. Government Printing Office, Washington 25, D. C., 1961).
[21] L. I. Schiff, Phys. Rev. **83**, 252 (1951).
[22] H. W. Koch and J. W. Motz, Rev. Mod. Phys. **31**, 920 (1959).

6. Detection Efficiency ε

The efficiency of the counting system was checked frequently during the experiment by counting for a standard count period the annihilation radiation from a Na^{22} source. Data were later corrected for changes in the counting efficiency detected in this manner. Changes resulting from the decay of the Na^{22} source were taken into account.

In addition to counting efficiency checks, data were taken at frequent periodic intervals at 36.00 MeV as a check on drift of all equipment in the experiment. Also, at intervals during the experiment, electrons from a Sr^{90} source were directed into the active volume of the monitor ionization chamber as a check on the stability of the entire beam monitor system.

III. ABSOLUTE CROSS-SECTION MEASUREMENT

For absolute calibration a sample smaller than the beam was bombarded at 50 MeV and subsequently counted in a 4-in.×4-in. well-type NaI(Tl) scintillation counter.[23] The absolute efficiency of the counter (88%) was calculated using a Fortran program written by Dingus and Stewart.[24] The error in the derived efficiency is believed to be less than 2%. For this calibration the activity computer was not used; instead the charge collected in a 3-min bombardment was used for dosimetry. The integrating capacitor was 0.10 μF as determined from a measurement at 1000 cycles using a recently calibrated impedance bridge.[25] A direct-current method for determining the capacitance gives the same result within the accuracy of the 1000-MΩ charging resistor (5%). A deliberate attempt was made to keep the beam intensity constant during these bombardments so that the induced activity would be proportional to the integrated dose. The measured dose was corrected to the results of Pruitt and Domen[16] using the measured angular distribution of the beam, beam absorption in the sample, and use of dry nitrogen at positive pressure in the chamber instead of air at STP. The yield of O^{16} was corrected for the decay of O^{15} during bombardment and the delay before counting, the finite counting time, extraneous activities, and counting losses. The yield was 5.92×10^{-29} (O^{15} atoms) cm^2/MeV (O^{16} atoms) at 50 MeV. The absolute yield at energies other than 50 MeV is shown in Fig. 2.

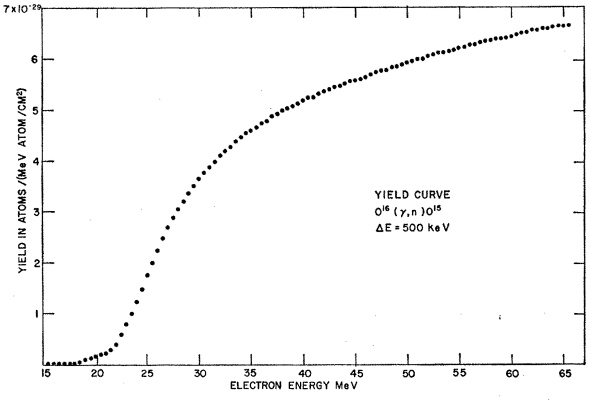

FIG. 2. The $O^{16}(\gamma,n)O^{15}$ yield function. The accuracy in absolute yield is ±7%. The relative accuracy except at low energy is ±0.14%.

[23] We are indebted to A. J. Voigt for use of this crystal.
[24] R. S. Dingus and M. G. Stewart, U. S. Atomic Energy Commission Report IS-606, 1961 (unpublished).
[25] General Radio Type 650 A.

IV. DATA HANDLING

Points on the yield curve were measured at 220 energies between 15.5 MeV and 65.5 MeV. Two separate experiments were performed under slightly differing conditions several weeks apart. Both sets of measurements consisted of a minimum of 3 measurements of yield points at each energy. As over 3300 runs were made, data for each energy point were typed on an IBM card for later processing by a computer. However, the yield was also calculated using only sample-normalization corrections during the course of the experiment. Thus a rough check on the quality of the data was available as the experiment progressed.

The computer output was a corrected yield point for each run, the averaged yield Y_i at each energy E_i, an estimate ϵ of the reproducibility of the data expressed as a fractional error independent of energy, an error estimate ΔY_i for each point derived from ϵ and the counting statistics, and the normalized residuals for each run, i.e., $(Y_i(E_i)-\overline{Y}_i(E_i))/\Delta Y_i$. The corrections applied are shown in Table I. For the first set of data ϵ was 0.31%, and for the second set it was 0.37%. The accuracy of our yield curves (neglecting counting statistics, which were unimportant except at the lowest energies) is 0.14%. From these measurements three yield functions were obtained: (1) Giant resonance energy region: 15.5 → 30.375 MeV in intervals of 0.125 MeV. (2) Intermediate energy A: 15.5 → 45.25 MeV in intervals of 0.25 MeV. (3) Intermediate energy B: 15.5 → 65.5 MeV in intervals of 0.5 MeV.

Because cross sections are related to the derivatives of yield functions, they are quite subject to localized errors in the yield functions. Such errors can produce

TABLE I. Maximum corrections applied to data. Background = 1500/(3 min).

	Set 1 (%)	Set 2 (%)
Count rate dependence	3	4
Time-dependent correction	0.5	1.7
Sample normalization	1	1
Curve normalization	0.1	0.1
Sample transmission	15	15
Extraneous activities	1.5	1.5

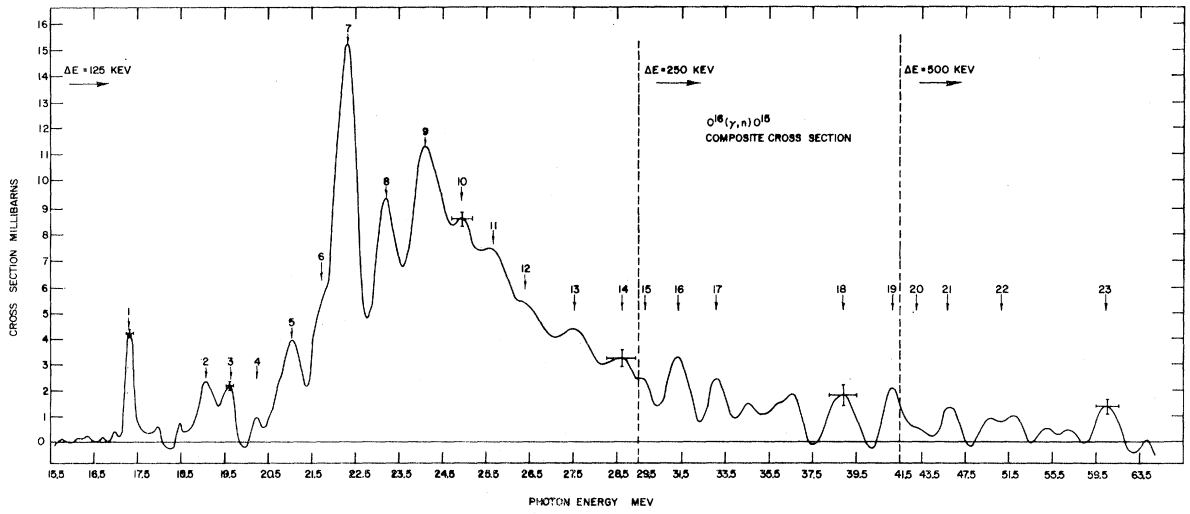

FIG. 3. The $O^{16}(\gamma,n)O^{15}$ cross section for energy to 65 MeV. This curve represents a fully converged least-structure solution for the yield function obtained using the average of six independent measurements. From 15.5 to 29.5 MeV data were taken in 125-keV intervals, from 29.5 to 41.5 MeV in 250-keV intervals, and above 41.5 MeV in 500-keV intervals. The vertical bars represent the standard deviation for the solution at representative energies. However, as adjacent cross-section points are strongly correlated, the interpretation of this bar as a random error is erroneous. The horizontal bar is the full width at half-maximum of the least-structure resolution function at representative energies. The numbered peaks occurred consistently in all cross sections derived from individual yield functions.

apparent resonances in the derived cross section curve. Anomalous structure might arise from two sources, namely imprecision (1) in the yield functions or (2) in the analysis of the yield functions for cross section. The extensive precautions to ensure the validity of $Y(E_i)$ were explained earlier. The reproducibility of the structure among the various runs ensures that its origin is not statistical.

However, structure might arise from valid yield functions in the analysis of these functions for the cross sections.

Bremsstrahlung Spectrum Effect

Since the bremsstrahlung spectrum occurs as the kernel of the integral equation [refer to Eqs. (1)–(5) relating $\sigma(k)$ to $y(E_0)$], deviations of the assumed Schiff integrated-over-angle spectrum from the true thin-target bremsstrahlung spectrum will cause errors in the derived cross sections. The Schiff spectrum was chosen primarily as a matter of convenience, but *a posteriori* support for the choice is possible, namely the reasonable shape of the sharp cross-section resonance at 17.28, Fig. 3. No evidence for "overshoot" or a "tail" is found. The following factors lead to the initial selection of this spectrum: (1) Most photonuclear yield curves have been analyzed using Penfold-Leiss tables[9] based on this spectrum. (2) The Schiff spectrum is an analytic formula in all energy ranges. (3) Although the Schiff formula is based on Born approximations implying zero cross sections for the highest photon energy (the tip), the tip cross section is finite as a result of certain analytical approximations. The bremsstrahlung cross section is now known to be finite at the tip.[26] (4) The experimental cross section follows the Schiff spectrum quite closely for photon energies away from the tip. (5) Finite-target effects will reduce the number of photons in the tip below the thin-target results, so that the Schiff formula might better represent the experimental spectrum at high energy than an exact formula near the tip.

To investigate the effect of spectrum shape upon cross sections several choices for the spectrum were made. In the first case, the spectrum was modified to correspond to more photons at the tip. The spectrum was taken to be linear at high energies joining the Schiff spectrum at lower energy with a continuous slope. The straight-line portion extended to a theoretical tip value.[27] This spectrum contained approximately 50% more photons in the highest energy interval. All structure in the cross section found using the Schiff spectrum was reproduced using the modified spectrum. However, the sharp peak at 17.28 MeV was less symmetrical using the modified spectrum, with a definite "tail" indicating that the latter spectrum had an excess of high-energy photons. A second change in the effective spectrum was tried by purposely calculating the spectrum for an energy 11 MeV higher than each datum. Again the structure was unchanged, although the absolute values were in this case meaningless.

---

[26] H. E. Hall, A. O. Hanson, and G. D. Jamnik, Phys. Rev. **129**, 2207 (1963).

[27] R. T. Deck, C. J. Mullin, and C. L. Hammer, Nuovo Cimento **32**, 180 (1964).

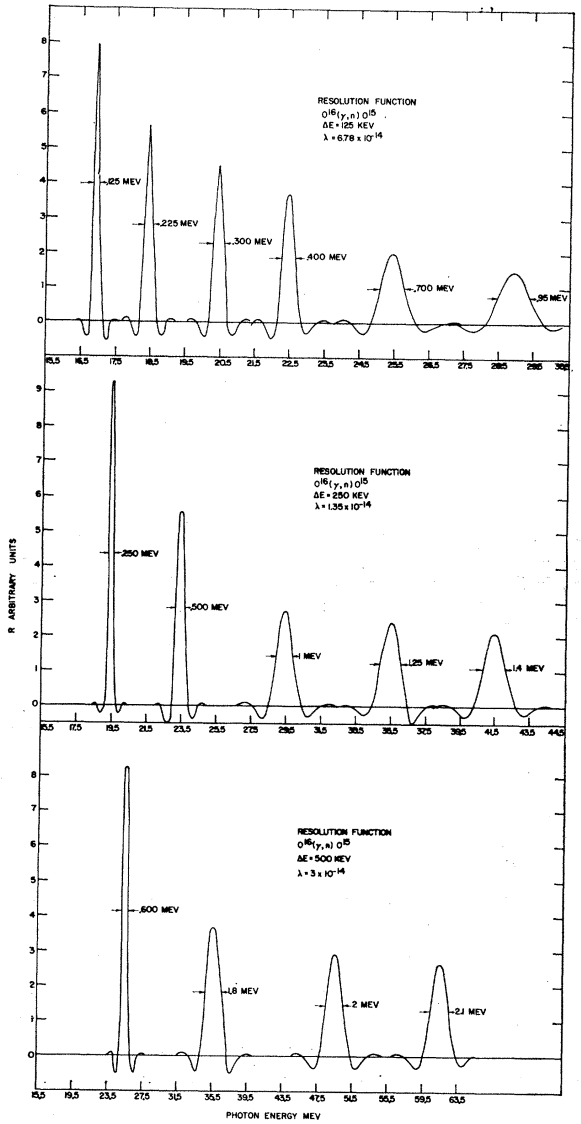

FIG. 4. The least-structure resolution function at representative photon energies for 125-, 250-, and 500-keV-interval data. One such function is obtained at each energy for which a yield point is measured. The least-structure cross section at a photon energy k is the true physical cross section weighted by the resolution function for the energy k. The effective resolution is taken as the full width at half-maximum of these functions at each energy. While the resolution functions "overshoot" to some extent, the resulting oscillation quickly damps away from the nominal energy to which it is assigned. Thus the observed structure can not be due to least-structure analysis.

Data Correction Factors

Discontinuity in slope in the yield function will give structure in the derived cross section. Before an experimental yield function may be analyzed for the cross section, many correction factors must be applied to the data. To ensure that no discontinuities arise from these factors, all corrections were smoothed to remove slope discontinuities.

Least-Structure Analysis

The smoothing implicit in the least-structure method could conceivably give rise to false structure; however, the method gives resolution functions as well as cross sections and errors. Typical resolution functions for 125-, 250-, and 500-keV data are shown in Fig. 4. While some "overshoot" is apparent in these typical resolution functions, the resultant oscillations damp out quite quickly and are too small to give the observed structure. A more detailed discussion of the resolution functions implied by the least-structure method is contained in a paper mentioned previously.[10] As a further check the photoneutron cross sections for Pr^{141} and C^{12} have also been measured in this laboratory. While both cross sections appear to have structure in the giant resonance, the $Pr^{141}(\gamma,n)Pr^{140}$ reaction is structureless above 20 MeV, while the $C^{12}(\gamma,n)C^{11}$ cross section is essentially structureless above 40 MeV. In the giant resonance the C^{12} and the Pr^{141} cross sections do not resemble that of O^{16}. Thus the structure reported here is characteristic of O^{16} and is not an experimental anomaly of the accelerator or other associated equipment. Details about the use of the least-structure method for the analysis of yield curves generated from experimental data will be given in another paper.[28]

V. RESULTS

The $O^{16}(\gamma,n)O^{15}$ cross section from 15.5 to 65 MeV is displayed in Fig. 3. In this figure the energy scale changes at 41.5 and 29.5 MeV. Prominent structure is seen both in the giant-resonance region ($\sim$24 MeV) and at higher energy. At several representative energies the error $\Delta\sigma$ is shown as a vertical bar and the experimental resolution by a horizontal bar. The latter is the full width at half-maximum of the resolution function given by the least-structure solution.

All labeled structure on the cross-section curve is considered to represent structure in the O^{16} cross section. As the yield at most energies was measured six times in two counters, 12 separate yield curves were obtained. The average yields for each counter for the two independent runs were analyzed as well as the average of all points. In this way four individual cross section curves were obtained. Our criterion for the statistical validity of structure is that it must appear in all four individual curves. Thus the structure near 35.5 MeV is suspect although it was present in three of the four individual curves.

As a further check of the statistical significance of structure, the yield was computed from a cross-section curve obtained by smoothing out one high-energy resonance. The smoothed cross section had the same integrated cross section as the original curve. The modified yield function deviated significantly from the measured yield in a correlated way. Thus the modified cross

[28] B. C. Cook (to be published).

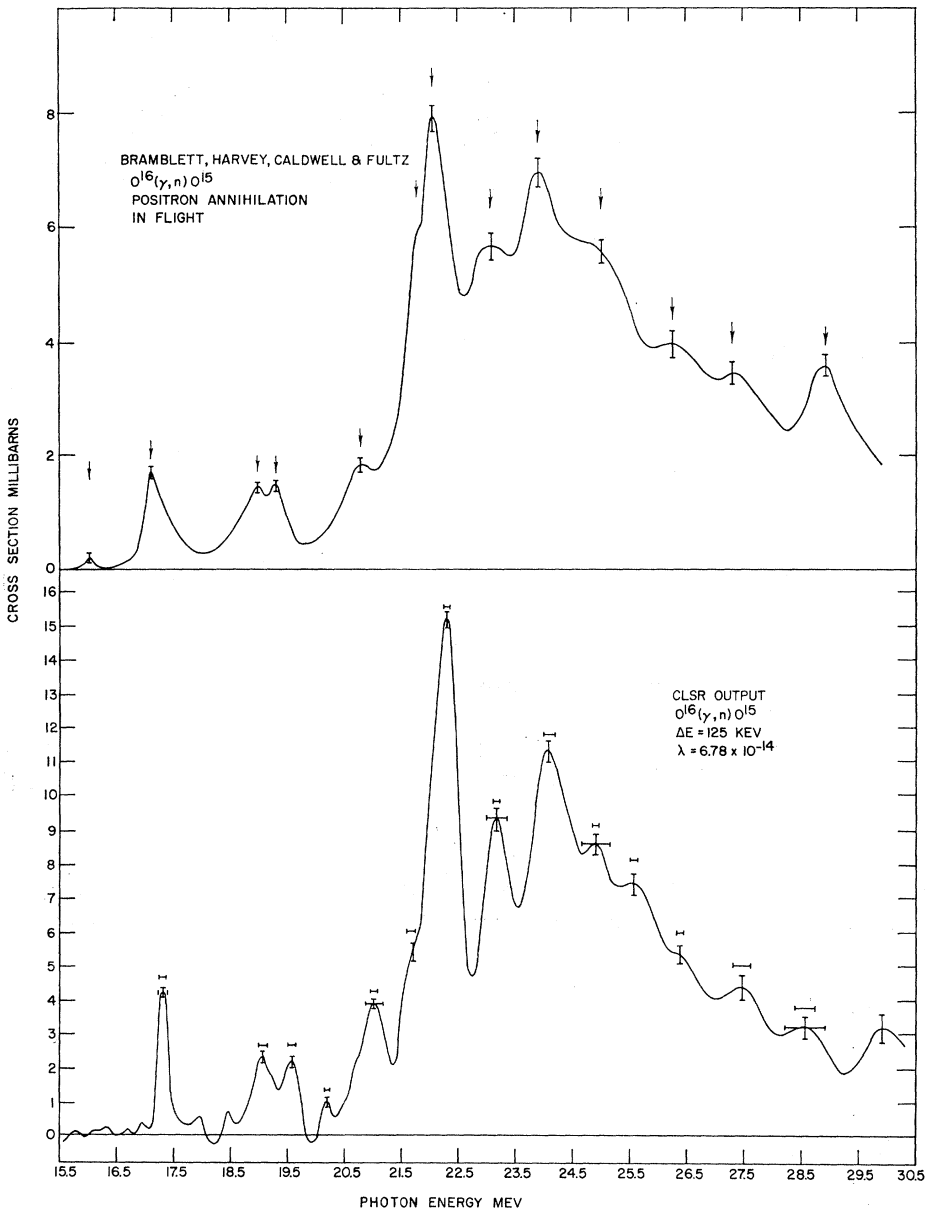

FIG. 5. The $O^{16}(\gamma,n)O^{15}$ cross section in the giant resonance. Data obtained using monoenergetic photons from positron annihilation in flight are also shown. In this figure the vertical and horizontal bars centered on the curve have the same interpretation as in Fig. 3. The horizontal bars are a measure of the reproducibility of peaks in cross sections derived from individual runs. In general, the agreement between the two measurements with respect to energies of the structure is good, but the absolute integrated cross sections differ by 20%. Since the resolution is not comparable, peak cross sections should not be compared. CLSR refers to least-structure computer routine.

section was not an acceptable solution to the experimental data. Yield functions were also computed from simulated cross-section curves without structure above the giant resonance. Errors comparable to the experimental error were assigned to the simulated yield in a random manner. While the cross section derived from these simulated experimental yields was not structureless, all features were smaller than the structure reported here. More significantly, no correlation was found among curves using differing sets of random errors. In contrast, the structure reported here was highly correlated in independent-yield curves.

1. Giant Resonance

In Fig. 5 are displayed our results as well as a recent measurement made by Bramblett, Caldwell, Harvey, and Fultz[15] using monoenergetic gamma rays (positron-annihilation method). In the latter experiment the (γ,pn) reaction is measured above 22.96 MeV as well as the (γ,n) reaction. This fact may account for the differing shape at higher energy between the two works. The vertical error bars represent the error as determined from the reproducibility of our data, while lower horizontal bars are the resolution using the full width at half maximum of the resolution function. The smaller horizontal bars are an estimate of the error in the

TABLE II. Resonances observed in O^{16}.[a]

Peak number (Fig. 3)	Present work (γ,n) E (MeV)	Error (keV)	% of $\int_{15.5}^{62}\sigma dE$	Bramblett *et al.* (γ,n) E M(eV)	Firk (γ,n) E (MeV)	Tanner *et al.* (p,γ_0) E (MeV)	Morrison *et al.* (γ,p) E (MeV)	Barber and Dodge (e,pe') E (MeV)	Griffin (γ,n) E (MeV)
1	17.30	±30	1.2	16.0, 17.1	17.1, 17.3	16.18, 17.13, 17.29	17.3	17.27	
2	19.06	60	1.3	19.0	19.0	19.05	19	18.07, 18.99	
3	19.56	100	1.1	19.3	19.4	19.56	19.6	19.57	
4	20.20	150	...		20.1		...		
5	21.0	30	3.7	20.8	20.9	21.0	20.7	20.65	
6	21.7	30	...	21.8	21.6		21.7		
7	22.26	38	15.6	22.1	22.1, 22.3	22.2	22.3	22.3	
8	23.15	34	5	23.1	23.1	23.0	23	23.1	
9	24.1	170	20	24.0	24.1, 24.3	24.3	24.3	24.35	
10	24.9	210	3	25.0			25		
11	25.55	50	6			25.2	25.5		
12	26.38	180	2	26.2			26.3		
13	27.45	230	4	27.3			27.4		
14	28.55	195	3	28.9					
15	29.6	230	0.5						
16	31.4	140	4						
17	33.0	300	3						33.0
18	38.75	170	2						39.7
19	41.1	170	2						
20	43.0	380	2						
21	46.0	470	3						45.9
22	51.0	960	4						51.6
23	60.2	150	3						58.4

[a] Integrated cross section: $\int_{15.5}^{30}\sigma dE = 58 \pm 6$ MeV mb; $\int_{15.5}^{62}\sigma dE = 81 \pm 8$ MeV mb.

position of the peak as determined from the reproducibility of peaks in the four individual cross-section curves described previously. The over-all agreement in shape between the two experiments is excellent. The integrated cross section to 30 MeV is 58 MeV mb, compared with the monochromatic-photon result of 46±5 MeV mb. The peak at 17.28 in our data was used to determine our energy scale. Bramblett *et al.* give this energy as 17.1 MeV. In general, the energies reported in this paper are above those given by Bramblett *et al.* below 25 MeV. This is a result of our choice for the energy calibration. However, the consensus in most reports is that this peak should be near 17.3 MeV. Other recent measurements give 17.31,[12] 17.29,[29] and[30] 17.27 MeV.

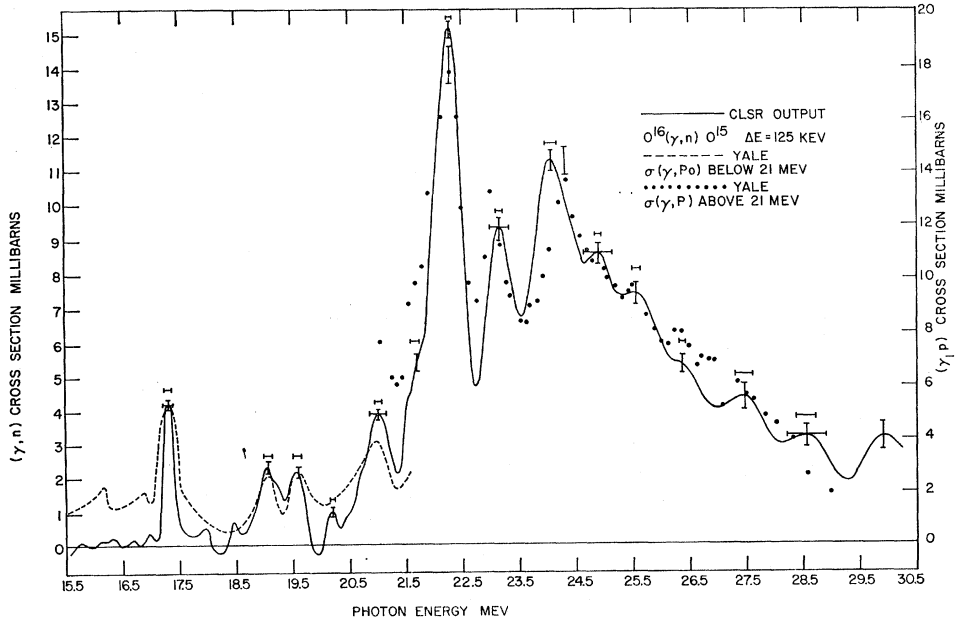

FIG. 6. A comparison between the (γ,p) and (γ,n) reaction in O^{16}. A recent measurement at Yale of the (γ,p) cross section obtained from the proton energy distribution is compared with results reported here. The scale on the left refers to the $O^{16}(\gamma,n)O^{15}$ cross section, while the scale on the right refers to the $O^{16}(\gamma,p)N^{15}$ cross section. The agreement between the cross sections for these differing processes is excellent.

[29] N. W. Tanner, G. C. Thomas, and E. D. Earle, Nucl. Phys. **52**, 45 (1964).
[30] W. R. Dodge and W. C. Barber, Phys. Rev. **127**, 1746 (1962).

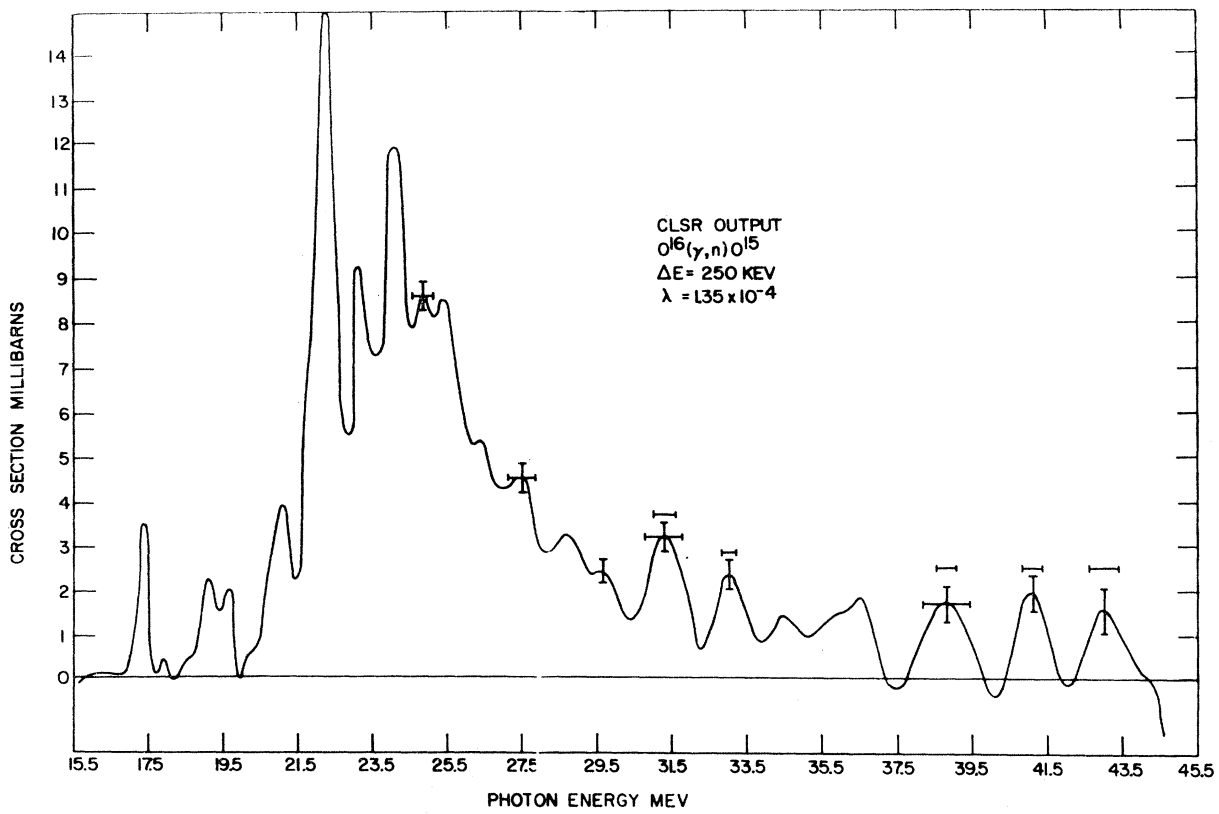

FIG. 7. The $O^{16}(\gamma,n)O^{15}$ cross section to 45 MeV. For the meanings of the symbols see Figs. 3 and 5.

Thus the energy discrepancies below 25 MeV may be explained. Above 25 MeV our data give results at a somewhat lower energy than those of Bramblett *et al.* Since the errors are large in both experiments in this region, these differences are insignificant. The additional discrepancy in peak cross section represents the somewhat improved resolution in this work.

Recent measurements using bremsstrahlung have obtained 64±7 MeV mb to 35 MeV [31] and 61±7 MeV mb to 33 MeV.[32] Our result is 65±7 MeV mb to 35 MeV.

In Table II the energies of cross-section peaks are compared with a few of the more recent higher resolution measurements in the giant-resonance region of O^{16}. The table includes measurements using monochromatic photons,[15] measurements of the photoneutron reaction by neutron time of flight,[12] photoproton energy distribution,[30,33] and a result using the $O^{15}(p,\gamma_0)O^{16}$ reaction.[29] The general features of all experiments are in good agreement for both the (γ,p) and $\gamma,n)$ reactions. The resolutions of all five experiments are comparable except for the (p,γ_0) experiment, which shows much superior resolution. In three experiments, peaks are found below 17.3 MeV which are not reported in this work. At these energies the intensity of our accelerator is insufficient to give an adequate yield. In earlier work[19,34,35] breaks in activation curves have been reported at 16.1, 17.13, and 17.3 MeV, so that these lower energy peaks are certainly valid. The agreement in energies and cross-section shape with the results of Morrison *et al.*[33] $(\gamma,p$ spectra) and those of[29] Tanner *et al.* (p,γ_0) is especially good. The former is displayed in Fig. 6. These results, produced by totally independent techniques, lend added credence to the energy scale used in this work. The peak at 20.2 MeV appears only in this work and in the report by Firk.[12] The peak, though very small, appeared in all individual curves and is probably valid. The peak at 29.6 MeV has been reported in no other experiment, probably because high-resolution work has been concentrated mainly on lower energies.

2. Cross Section above the Giant Resonance

The cross section for $O^{16}(\gamma,n)O^{15}$ from 15.5 to 65 MeV is shown in Figs. 7 and 8. Figure 7 gives data taken in 260-keV intervals and Fig. 8 gives data for 500-keV intervals. In addition to the 15 cross-section peaks below 30 MeV, eight peaks above 30 MeV are also found. Evidence corroborating this structure is still fragmentary, although some structure in this energy

[31] G. R. Bishop, B. Grossetête, and J. Risset, J. Phys. Radium **23**, 31 (1962).
[32] P. Brix, H. Fuchs, K. Lindenberger, and C. Salander, Z. Physik **165**, 485 (1961).
[33] R. C. Morrison, J. R. Stewart, and J. S. O'Connell, Bull. Am. Phys. Soc. **10**, 95 (1965).
[34] J. King and L. Katz, Can. J. Phys. **37**, 1357 (1959).
[35] A. S. Penfold and E. L. Garwin, Phys. Rev. **115**, 420 (1959).

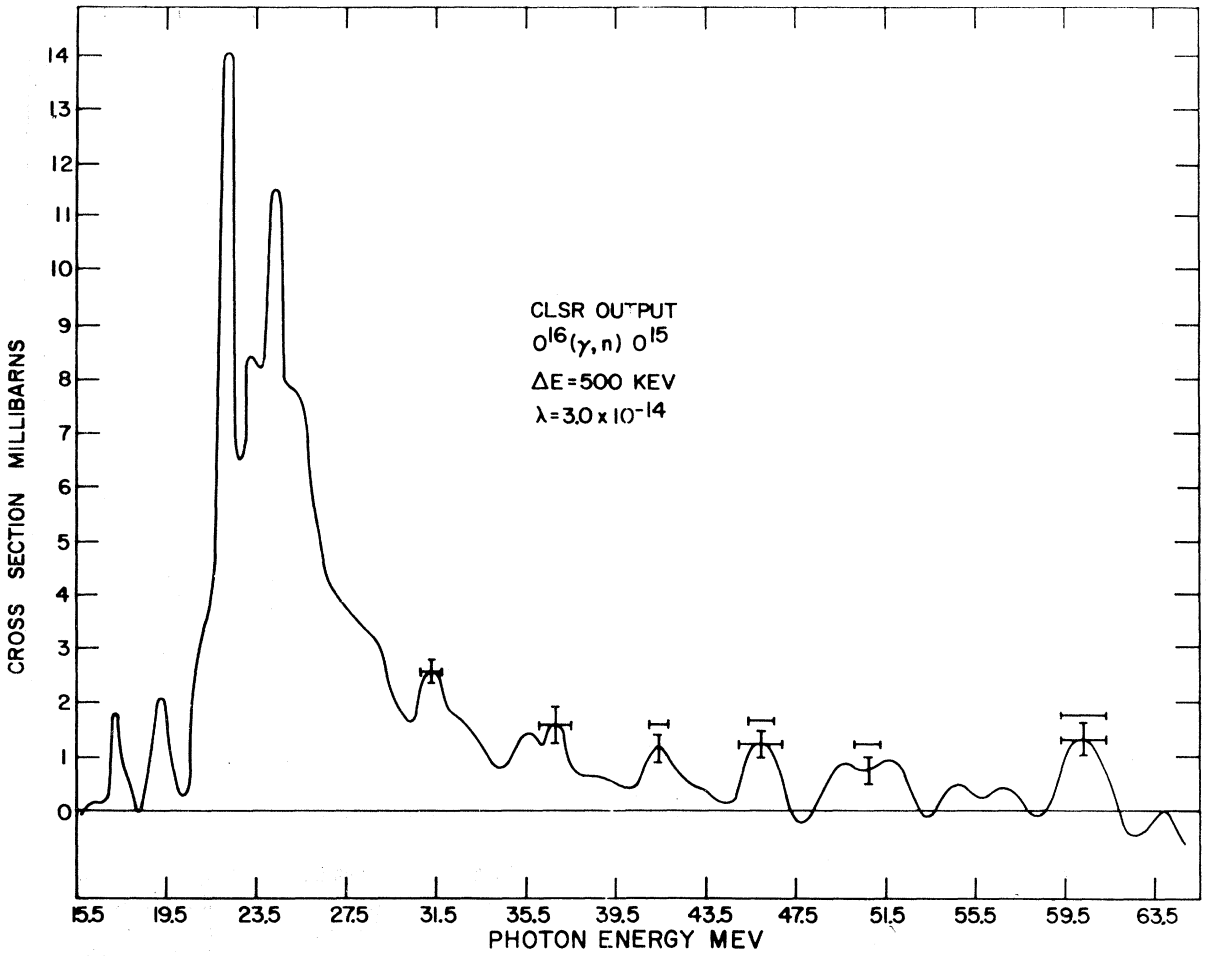

FIG. 8. $O^{16}(\gamma,n)O^{15}$ cross section to 65 MeV. Above 43 MeV the structure agrees with structure previously reported by this laboratory Between 37 and 44 MeV the resolution shown in Fig. 5 is superior. However, most features found in Fig. 5 have less prominent counterparts in this curve.

region has been reported previously. In a preliminary report of this work[11] structure in the $O^{16}(\gamma,n)O^{15}$ cross section was reported at 33±0.5, 39.7±0.5, 45.9±0.8, 51.6±0.8, and 58.4 MeV. The 33-MeV structure was an unresolved shoulder extending from 30 to 34 MeV which is resolved into two peaks (31.4 and 33.0 MeV) in this work. The single peak at 39.7 MeV is resolved into two peaks (38.8 and 41.1 MeV) in this work. The three highest energy peaks are consistent to within experimental error, although the peak at 43.0 MeV reported here occurs at a minimum in the earlier report and there appears to be a clear inconsistency between the two experiments. However, the 45.9-MeV resonance seemed to be asymmetrical in the previous paper, perhaps reflecting the effect of this resonance. The peak at 43.0 MeV was clearly resolved only in the 250-keV data, although its presence was reflected as well in the 500-keV data of the latest experiment. Since this peak is quite near the high-energy limit of the 250-keV yield curve, where least-structure analysis is least reliable, its validity is questionable, although it was present in all individual curves. The two experiments differ primarily in the reproducibility of yield points. In the original experiment, data were reproducible to 0.9%, corresponding to an accuracy of 0.53% for the average curve (3 curves), while in this experiment, the reproducibility was 0.35%, corresponding to an accuracy of 0.14% for the average of the six individual curves. Since the errors were larger in the first experiments, more smoothing was required. The necessity for more smoothing is reflected in the resolution functions for each experiment. At 60 MeV the resolution (full width at half maximum) was 3 MeV for the earlier paper and is 2 MeV in this work. In most cases the structure in O^{16} above the giant resonance has been confirmed in this work, although in two cases peaks reported earlier have been further resolved. Further improvements in experimental technique will certainly resolve more high-energy structure, just as high-resolution experiments have revealed many details in the giant resonance which were unresolved in pioneer photonuclear experiments.

No measurements with sufficient resolution to con-

firm all structure have been reported. However, using inelastic electron scattering Isabelle and Bishop[36] have reported peaks at 44.8 and 49.3 MeV. These may correspond to structure reported here at 46.0±0.5 and 51.0±1.0 MeV.

VI. DISCUSSION

1. Giant-Resonance Region

The very good agreement between the results of this experiment and the results of the photoproton experiments done at Yale,[33] Fig. 6, again confirms the observation[29] that (γ,n) and (γ,p) cross sections in O^{16} are similar.

The particle-hole model of Brown and others has been applied with considerable success to states in O^{16}. The use of empirical energies for the diagonal matrix elements of the Hamiltonian and the elevation of energy in collective states implicit in the model give qualitative agreement of theory with energies of experimental levels. The most striking agreement is in the two strong $E1$ transitions at about 22 and 24 MeV, appearing in both the theory and experiment. In these experiments the integrated cross section of the 22.26 and 24.1 MeV levels is 55% of the total integrated cross section to 30 MeV. In the particle-hole theory these two levels carry 95% or more of the dipole oscillator strength, so that the theory overestimates the experimental strength. Moreover in this experiment the ratio of the integrated cross section of the 24.1-MeV peak to that of the 22.26-MeV peak is 1.3. In all particle-hole calculations made to date this ratio is about 0.5 depending somewhat upon the potential mixture used.

Gillet[37] reports 15 1^-, $T=1$; 2^+, $T=0$; and 2^+, $T=1$ levels in O^{16} between 17 and 30.2 MeV. Of course 1^+ states not given by Gillet should also contribute structure in this energy region. Unfortunately this experiment gives no information about spin assignments, so that a detailed comparison of the levels with the calculation is unjustified. Spin and parity assignments have been given for a few of the levels but the experimental situation is as yet incomplete. Thus in contrast to other nuclei such as Si^{28} and Ca^{40}, the observed number of levels in O^{16} is comparable to the number predicated by particle-hole theory.

Unfortunately the transition probabilities calculated using particle-hole theory for many of these states are too small to correspond to transitions observed experimentally. A more serious discrepancy lies in the angular distribution in (p,γ_0) experiments. These distributions do not differ markedly from level to level, indicating that most transitions are of the same type. This uniformity of angular distribution has led the Argonne group[38] to conclude that all structure in the giant resonance is basically the same, reminiscent of a collective Teller-Goldhaber giant resonance split by residual nuclear forces into intermediate structure.

2. Above the Giant Resonance

The integrated cross section for the particle-hole model will exhaust the entire dipole-sum-rule value[39] of $60(NZ/A)(1+0.8x)$ with $x\approx 0.5$. Experimentally the integrated cross sections fall short of this sum by a large factor. This fact alone indicates that states other than the simple particle-hole states contribute substantially to the total photonuclear cross section. In this experiment we find an integrated cross section of 58 MeV mb to 62 MeV. The total integrated cross section is given as 150 MeV mb to 30 MeV in a recent photon absorption measurement.[40] Thus the high-energy cross section must be substantial between 30 MeV and the photomeson threshold. One known mechanism for high-energy absorption is the quasideuteron photoexcitation.[5,6] Other proposed mechanisms are harmonics of the giant resonance[7,8] and single-particle excitation of inner-shell nuclear levels.[37]

Quasideuteron photoexcitation will not show structure, while the observed cross section has strong structure between 30 MeV and 65 MeV. This is strong evidence that a mechanism other than quasideuteron photoexcitation is present. Both single-particle excitation and nuclear overtones may produce structure.

(1) Single-particle transitions: Shell-structure effects corresponding to s protons have been traced in $(p,2p)$ experiments[41] and in (e,pe') experiments[42] for elements up to Al. While the observed structure is broad (~14 MeV in O^{16}) the experimental widths may not represent the actual energy spread of the s-state nucleons. Gillet has shown that in the particle-hole picture, the s-d $E2$ transitions should be relatively large, have energies near 50 MeV, and be almost exclusively of single-particle nature.

(2) Using the hydrodynamical model, Danos[8] has predicted $E1$ overtones of the Teller-Goldhaber resonance at $2.86E_m$, and $E2$ overtones at $1.6E_m$. Carver and Peaslee[7] have examined the energy shifts in these predictions relative to the shell-model expectation. They give the $3\hbar\omega$ $E1$ overtone as $E_{3m}=(115A^{-1/3}+3)$ MeV or about 48 MeV for O^{16}. Thus both single-particle transitions and collective overtones are expected in O^{16} at energies comparable to transitions reported here. In the former case the levels would be 2^+ states, while if collective the levels are 1^-. Thus there is no difficulty in understanding the presence of high-energy structure in O^{16}, but a detailed comparison of the experiment with these theories is premature.

[36] D. B. Isabelle and G. R. Bishop, J. Phys. Radium **22**, 548 (1961).
[37] V. Gillet, Centre d'Etudes Atomique Report No. CEA 2177, 1962 (unpublished).
[38] R. G. Allas, S. S. Hanna, L. Meyer-Schützmeister, R. E. Segel, P. P. Singh, and Z. Vager, Phys. Rev. Letters **13**, 628 (1964).
[39] J. S. Levinger and H. A. Bethe, Phys. Rev. **28**, 115 (1950).
[40] J. M. Wyckoff, B. Ziegler, H. W. Koch, and R. Uhlig, Phys. Rev. **137**, B576 (1965).
[41] H. Tyren, P. Hillman, and Th. A. J. Maris, Nucl. Phys. **7**, 10 (1952).
[42] U. Amaldi, Jr., G. Campos Venuti, G. Cortellessa, G. Fronterotta, A. Reale, P. Salvadori, and P. Hillman, Phys. Rev. Letters **13**, 341 (1964).